Inorganica Chimica Acta, 215 (1994) 165–172

Synthesis and fluxional behaviour of (cyclopentadienyl) and (pentamethylcyclopentadienyl)ruthenium(II) complexes with hemilabile ether-phosphines. ^{31}P DNMR spectroscopic studies and line shape analysis

Ekkehard Lindner**, Michael Haustein, Hermann A. Mayer and Hartwig Kühbauch
Institut für Anorganische Chemie der Universität Tübingen, Auf der Morgenstelle 18, D-72076 Tübingen (Germany)

Kees Vrieze** and Barbara de Klerk-Engels
Anorganisch Chemisch Laboratorium, Universiteit van Amsterdam, Nieuwe Achtergracht 166, 1018 WV Amsterdam (Netherlands)

(Received June 22, 1993; revised August 12, 1993)

Abstract

A series of Cp*RuCl(P ~ O)$_2$ complexes (**3a–e**) (Cp* = η^5-C$_5$Me$_5$) were prepared *in situ* by reaction of [Cp*RuCl$_2$]$_n$ (**1**) with the ether-phosphine ligands Ph$_2$PCH$_2$–D (**2a–e**) (D = CH$_2$OCH$_3$ (**a**), 1,3-dioxolane-2-yl (**b**), 1,3-dioxane-2-yl (**c**), 1,3-dioxepane-2-yl (**d**), tetrahydrofuran-2-yl (**e**)) in the presence of zinc. Treatment of **3a–e** and CpRuCl(P ~ O)$_2$ (**4b,c**) with AgSbF$_6$ and NaBPh$_4$, respectively, afforded cationic, monochelated ruthenium(II) complexes of the type [(η^5-C$_5$R$_5$)Ru(P ~ O)(P$\frown$O)]$^+$ (**5a–e**: R = CH$_3$; **6b,c**: R = H). The fluxional behaviour of **5a–e** and **6c** was studied by temperature dependent ^{31}P NMR investigations. In the case of **5a–e** computer-generated spectra were fitted to the experimental by using DNMR5. Thermodynamic parameters $\Delta H^{\neq}$, $\Delta S^{\neq}$ and $\Delta G^{\neq}$ were obtained via graphic application of the Eyring equation to the kinetic data. Stirring **5c**, **6c** under an atmosphere of carbon monoxide results in the formation of [(η^5-C$_5$R$_5$)Ru(CO)(P ~ O)$_2$][SbF$_6$] (**7c**: R = CH$_3$; **8c**: R = H).

Key words: Ruthenium complexes; Cyclopentadienyl complexes; Ether-phosphine complexes

Introduction

Half-sandwich (cyclopentadienyl)ruthenium(II) systems have been reported as an excellent organometallic auxiliary in the investigation of catalytic processes [1]. In fact easy replacement of both the chloride and the phosphines in CpRuCl(PPh$_3$)$_2$ [2] has led to a variety of new metal complexes [3–5]. Recently an interesting study in our group has involved ether-phosphines (O,P) in complexes of this type [6]. The oxygen donors in the ether moiety of these ligands may be regarded as intramolecular solvent molecules forming only weak metal–oxygen bonds which may be cleaved reversibly (P ~ O: η^1-P coordinated; P$\frown$O: η^2-O,P coordinated) [7]. If the molecule is such that it allows the oxygen donor atoms which belong to different O,P ligands to compete for a common coordination site, fluxional behaviour can be observed [6–9]. Referring to this the first results about dynamic processes in octahedral ruthenium(II) [8] and square-pyramidal palladium(II) complexes [9] containing ether-phosphine ligands were published recently. Contributions of the various O,P ligands to the metal–oxygen bond strength were determined via ^{31}P DNMR spectroscopic studies.

Replacement of Cp with the more basic, electron donating pentamethylcyclopentadienyl (C$_5$Me$_5$) ligand has significantly affected the chemistry of organometallic ruthenium complexes [1, 10, 11]. Recent work by Bercaw and co-workers [11] and Suzuki and co-workers [12] has provided methodologies for the syntheses of Cp*RuClL$_2$ (L = tertiary phosphine) from oligomeric [Cp*RuCl$_2$]$_n$. The different properties of Cp* versus Cp in such systems is an area of active interest [13–16].

The present paper reports the synthesis, steric and spectroscopic properties of (cyclopentadienyl) and (pentamethylcyclopentadienyl)ruthenium(II) complexes provided with a series of ether substituents. The difference in reactivity of ionic complexes **5c** and **6c** with carbon monoxide is indicative for the change of the ruthe-

---

**Authors to whom correspondence should be addressed.

SSDI 0020-1693(93)03696-8

nium–oxygen bond strength by increase of electron density in the ruthenium centre via the Cp* ligand. The main attention is focused on the fluxional processes of **5a–e** and the activation parameters of the compounds are discussed.

Experimental

All manipulations were carried out under an atmosphere of argon by use of standard Schlenk techniques. Solvents were dried over appropriate reagents and stored under argon. IR data were obtained with a Bruker IFS 48 instrument. FD mass spectra were taken on a Finnigan MAT 711 A instrument (8 kV, 60 °C), modified by AMD. Elemental analyses were performed with a Carlo Erba 1106 analyzer; Cl and F analyses were carried out according to Schöniger [17] and analyzed as described by Dirschel and Erne [18] and Brunisholz and Michot [19]. Ru was determined according to the literature [20]. NMR spectra were obtained on a Bruker AC 80 spectrometer operating at 32.44 MHz for ^{31}P and 20.15 MHz for ^{13}C, or on a Bruker AC 250 instrument, operating at 101.38 MHz for ^{31}P and 62.90 MHz for ^{13}C. All ^{31}P and ^{13}C NMR spectra were proton-decoupled. ^{31}P chemical shifts were reported relative to external H_3PO_4 (85% in D_2O, 1% in acetone-d_6). ^{13}C chemical shifts were measured relative to partially deuterated solvent peaks which are reported relative to tetramethylsilane. The ^{31}P CP-MAS NMR spectrum was recorded on a Bruker MSL 200 multinuclear spectrometer with a wide-bore magnet (4.7 T), referenced to NH_4HCO_3. Magic angle spinning was performed at a 3.5 kHz spinning rate (297 K) in double-bearing rotors of ZrO_2.

^{31}P DNMR experiments were carried out on a Bruker AC 80 instrument. A 10-mm NMR tube was charged with ~50 mg of the complex and 2.4 ml of THF. Variable temperature ^{31}P NMR spectra were collected at 10 °C intervals in the temperature range between 181 and 325 K. Near coalescence temperatures, spectra were recorded at 2–5° intervals. The temperature was measured using a temperature control unit (VT 100 Bruker instrument) and an external thermocouple (PT 100). The NMR probe temperature was calibrated using the method of Van Geet [21] and is considered accurate to ± 1 K (about 20 min was required for the temperature equilibration of the NMR sample). All exchange broadened NMR spectra were simulated using DNMR5 [22] available from the Quantum Chemistry Program Exchange (QCMP 365). The analysis of the rate constant data was performed with ACTPAR [23], a non-linear least-squares program to fit the values of the desired parameters. Reported values are given with standard deviations.

Reagents

$[Cp^*RuCl_2]_n$ (**1**) was prepared as described by Suzuki and co-workers [12]. The ether-phosphines **2a–e** [24] and the complexes **4b,c** [6] were synthesized according to literature procedures.

General route to $Cp^*RuCl(P{\sim}O)_2$ complexes (3a–e)

To a solution of 700 mg (2.3 mmol) $[Cp^*RuCl_2]_n$ (**1**) in 60 ml of toluene, ether-phosphine ligands **2a–e** (7.0 mmol) and 800 mg (12.2 mmol) of zinc were added. After refluxing for 12 h the colour of the dark red reaction mixture had turned to bright yellow. Excess Zn and $ZnCl_2$, respectively, were separated by filtration. After evaporation of the solvent under reduced pressure, the product was purified by column chromatography using activated silica gel in a column of 3 × 25 cm. With n-hexane/diethyl ether = 5/1 as eluents the first fraction contained excess **2a–e**. The main fraction was eluated with n-hexane/diethyl ether = 1/1 and contained pure **3a–e**. A small amount of **1** still remained on the column. The solvent of the main fraction was removed in vacuum and **3a–e** were obtained as yellow powders.

$Cp^*RuCl(P{\sim}O)_2$ (3a)

3a was obtained in 50% yield, m.p. 94–96 °C (dec.). FD-MS: *m/z* 761 [M^+]. *Anal.* Calc. for $C_{40}H_{49}ClO_2P_2Ru$ (760.3): C, 63.19; H, 6.50; Cl, 4.66; Ru, 13.60. Found: C, 63.47; H, 6.73; Cl, 4.70; Ru, 13.29%. IR (KBr): $\nu_{as}(C_2O)$ 1105 cm^{-1}. ^{13}C NMR (62.90 MHz, $CDCl_3$, 22 °C): δ (ppm) 137.22–127.29 (m, C–Ph), 88.56 (s, C-η^5-Cp*), 69.71 (s, CH_2O), 57.82 (s, OCH_3), 26.00 (m, PCH_2), 9.24 (s, CH_3–Cp*).

$Cp^*RuCl(P{\sim}O)_2$ (3b)

3b was obtained in 60% yield, m.p. 99–101 °C (dec.). FD-MS: *m/z* 817 [M^+]. *Anal.* Calc. for $C_{42}H_{49}ClO_4P_2Ru$ (816.3): C, 61.80; H, 6.05; Cl, 4.34; Ru, 12.38. Found: C, 61.81; H, 6.19; Cl, 4.57; Ru, 11.70%. IR (KBr): $\nu_{as}(C_2O)$ 1114 cm^{-1}. ^{13}C NMR (62.90 MHz, $CDCl_3$, 22 °C): δ (ppm) 137.27–127.22 (m, C–Ph), 102.79 (s, CH), 88.43 (s, C–η^5-Cp*), 65.00, 64.18 (s, $O(CH_2)_2O$), 31.65 (m, PCH_2), 9.23 (s, CH_3–Cp*).

$Cp^*RuCl(P{\sim}O)_2$ (3c)

3c was obtained in 64% yield, m.p. 113–115 °C (dec.). FD-MS: *m/z* 845 [M^+]. *Anal.* Calc. for $C_{44}H_{53}ClO_4P_2Ru$ (844.4): C, 62.59; H, 6.33; Cl, 4.20; Ru, 11.97. Found: C, 62.75; H, 6.60; Cl, 4.27; Ru, 11.60%. IR (KBr): $\nu_{as}(C_2O)$ 1127 cm^{-1}. ^{13}C NMR (62.90 MHz, $CDCl_3$, 22 °C): δ (ppm) 137.28–126.92 (m, C–Ph), 101.40 (s, CH), 88.63 (s, C–η^5-Cp*), 66.92, 66.43 (s, OCH_2CH_2), 32.72 (m, PCH_2), 25.19 (s, OCH_2CH_2), 9.26 (s, CH_3–Cp*).

$Cp^*RuCl(P\sim O)_2$ (3d)

3d was obtained in 55% yield, m.p. 112–114 °C (dec.). FD-MS: *m/z* 873 [M^+]. *Anal.* Calc. for $C_{46}H_{57}ClO_4P_2Ru$ (872.4): C, 63.33; H, 6.59; Cl, 4.06; Ru, 11.59. Found: C, 63.38; H, 6.80; Cl, 4.43; Ru, 11.23%. IR (KBr): $\nu_{as}(C_2O)$ 1116 cm^{-1}. ^{13}C NMR (62.90 MHz, $CDCl_3$, 22 °C): δ (ppm) 137.57–126.90 (m, C–Ph), 100.61 (s, CH), 88.40 (s, C–η^5-Cp*), 65.65, 65.30 (s, OCH_2CH_2), 33.11 (m, PCH_2), 28.99, 28.90 (s, $OCH_2(CH_2)_2CH_2O$), 9.24 (s, CH_3–Cp*). ^{31}P CP-MAS NMR (81.0 MHz): δ (ppm) 39.3, 33.5 (s).

$Cp^*RuCl(P\sim O)_2$ (3e)

3e was obtained in 62% yield, m.p. 103–105 °C (dec.). FD-MS: *m/z* 812 [M^+]. *Anal.* Calc. for $C_{44}H_{53}ClO_2P_2Ru$ (812.4): C, 65.05; H, 6.58; Cl, 4.36; Ru, 12.44. Found: C, 64.97; H, 6.61; Cl, 4.34; Ru, 12.10%. IR (KBr): $\nu_{as}(C_2O)$ 1096 cm^{-1}. ^{13}C NMR (62.90 MHz, $CDCl_3$, 22 °C): δ (ppm) 139.47–127.14 (m, C–Ph), 88.67–88.15 (m, C–η^5-Cp*), 76.22–76.08 (m, CH), 67.29–66.51 (m, OCH_2), 37.37–29.67 (m, $OCH_2CH_2CH_2$, PCH_2), 25.75–25.16 (m, OCH_2CH_2), 9.42–9.22 (m, CH_3–Cp*).

General route to $[(\eta^5\text{-}C_5R_5)Ru(P\sim O)(P^\frown O)][SbF_6]$ complexes (5a–c, 5e, 6b,c)

To a solution of 300 mg **3a–c**, **3e**, **4b,c** in 15 ml of THF an equimolar amount of $AgSbF_6$ dissolved in 2–3 ml of THF was added. The mixture was stirred for 2 h at ambient temperature in the dark. The reaction mixture was separated from AgCl by centrifugation. After evaporation of the solvent, the residue was washed with 10 ml of n-hexane to give an orange precipitate. The precipitate was collected by filtration and dried under vacuum.

$[Cp^*Ru(P\sim O)(P^\frown O)][SbF_6]$ (5a)

300 mg (0.39 mmol) **3a** were reacted with 135 mg (0.39 mmol) $AgSbF_6$. **5a** was obtained in 82% yield, m.p. 97 °C (dec.). FD-MS: *m/z* 725 [M^+-SbF_6]. *Anal.* Calc. for $C_{40}H_{49}F_6O_2P_2RuSb$ (960.6): C, 50.01; H, 5.14; F, 11.89; Ru, 10.52. Found: C, 50.43, H, 5.52; F, 12.09; Ru, 11.09%. IR (KBr): $\nu_{as}(C_2O)$ 1100 (P ~ O), 1064 (P⌒O); ν(SbF) 658 cm^{-1}.

$[Cp^*Ru(P\sim O)(P^\frown O)][SbF_6]$ (5b)

300 mg (0.37 mmol) **3b** were reacted with 126 mg (0.37 mmol) $AgSbF_6$. **5b** was obtained in 85% yield, m.p. 121–123 °C (dec.). FD-MS: *m/z* 782 [M^+-SbF_6]. *Anal.* Calc. for $C_{42}H_{49}F_6O_4P_2RuSb$ (1016.6): C, 49.62; H, 4.86; F, 11.21; Ru, 9.94. Found: C, 50.14; H, 5.17; F, 11.80; Ru, 10.10%. IR (KBr): $\nu_{as}(C_2O)$ 1106 (P ~ O), 1070 (P⌒O); ν(SbF) 659 cm^{-1}.

$[Cp^*Ru(P\sim O)(P^\frown O)][SbF_6]$ (5c)

300 mg (0.36 mmol) **3c** were reacted with 122 mg (0.36 mmol) $AgSbF_6$. **5c** was obtained in 87% yield, m.p. 126–128 °C (dec.). FD-MS: *m/z* 810 [M^+-SbF_6]. *Anal.* Calc. for $C_{44}H_{53}F_6O_4P_2RuSb$ (1044.7): C, 50.59; H, 5.11; F, 10.91; Ru, 9.67. Found: C, 50.00; H, 5.14; F, 10.54; Ru, 9.62%. IR (KBr): $\nu_{as}(C_2O)$ 1123 (P ~ O), 1066 (P⌒O); ν(SbF) 658 cm^{-1}.

$[Cp^*Ru(P\sim O)(P^\frown O)][SbF_6]$ (5e)

300 mg (0.37 mmol) **3e** were reacted with 127 mg (0.37 mmol) $AgSbF_6$. **5e** was obtained in 82% yield, m.p. 108–110 °C (dec.). FD-MS: *m/z* 776 [M^+-SbF_6]. *Anal.* Calc. for $C_{44}H_{53}F_6O_2P_2RuSb$ (1012.7): C, 52.19; H, 5.28; F, 11.26; Ru, 9.98. Found: C, 51.51; H, 5.35; F, 11.72; Ru, 9.35%. IR (KBr): $\nu_{as}(C_2O)$ 1095 (P ~ O), 1066 (P⌒O); ν(SbF) 658 cm^{-1}.

$[CpRu(P\sim O)(P^\frown O)][SbF_6]$ (6b)

300 mg (0.40 mmol) **4b** were reacted with 138 mg (0.40 mmol) $AgSbF_6$. **6b** was obtained in 82% yield, m.p. 164 °C (dec.). FD-MS: *m/z* 711 [M^+-SbF_6]. *Anal.* Calc. for $C_{37}H_{39}F_6O_4P_2RuSb$ (946.5): C, 46.95; H, 4.15; F, 12.04; Ru, 10.68. Found: C, 47.61; H, 4.62; F, 12.31; Ru, 10.34%. IR (KBr): $\nu_{as}(C_2O)$ 1105 (P ~ O), 1069 (P⌒O); ν(SbF) 659 cm^{-1}.

$[CpRu(P\sim O)(P^\frown O)][SbF_6]$ (6c)

300 mg (0.39 mmol) **4c** were reacted with 134 mg (0.39 mmol) $AgSbF_6$. **6c** was obtained in 79% yield, m.p. 166 °C (dec.). FD-MS: *m/z* 739 [M^+-SbF_6]. *Anal.* Calc. for $C_{39}H_{43}F_6O_4P_2RuSb$ (974.5): C, 48.07; H, 4.45; F, 11.70; Ru, 10.37. Found: C, 47.66; H, 4.67; F, 12.21; Ru, 9.86%. IR (KBr): $\nu_{as}(C_2O)$ 1128 (P ~ O), 1075 (P⌒O); ν(SbF) 659 cm^{-1}.

Preparation of $[Cp^*Ru(P\sim O)(P^\frown O)][BPh_4]$ (5d)

To a solution of 300 mg (0.34 mmol) **3d** in 10 ml of CH_2Cl_2 118 mg (0.34 mmol) $NaBPh_4$ was added. The reaction mixture was stirred overnight at ambient temperature. After removal of the solvent under vacuum, the residue was redissolved in 20 ml of dichloromethane NaCl was separated by filtration over a fine filter (G4). CH_2Cl_2 was removed completely under vacuum. The residue was washed with 10 ml of n-hexane, collected by filtration (G3) and dried under reduced pressure to give **5d** as an orange powder in 97% yield, m.p. 100–102 °C (dec.). FD-MS: *m/z* 838 [M^+-BPh_4]. *Anal.* Calc. for $C_{70}H_{77}BO_4P_2Ru$ (1156.2): C, 72.72; H, 6.71; Ru, 8.74. Found: C, 71.87; H, 6.77; Ru, 8.29%. IR (KBr): $\nu_{as}(C_2O)$ 1117 (P ~ O), 1068 (P⌒O) cm^{-1}.

Preparation of $[Cp^*Ru(P\sim O)_2(CO)][SbF_6]$ (7c)

150 mg (0.14 mmol) **5c** were dissolved in 10 ml of dichloromethane and stirred under an atmosphere of CO. After 10 min the bright orange colour of the solution had turned completely into pale yellow. After removal of the solvent under vacuum, the residue was stirred in 10 ml of n-hexane. The pale yellow solid was

collected by filtration (G3) and dried under vacuum. Yield 82%, m.p. 108–110 °C (dec.). FD-MS: m/z 837 $[M^+ - SbF_6]$. *Anal.* Calc. for $C_{45}H_{53}F_6O_5P_2RuSb$ (1072.7): C, 50.39; H, 4.98; F, 10.63; Ru, 9.42. Found: C, 49.62; H, 5.00; F, 9.86; Ru, 9.39%. IR (KBr): ν(CO) 1946; ν(SbF) 658 cm^{-1}.

Preparation of $[CpRu(P \sim O)_2(CO)][SbF_6]$ (8c)

A solution of 120 mg (0.12 mmol) of **6c** in 15 ml of dichloromethane was stirred overnight under an atmosphere of carbon monoxide at ambient temperature. After this time the colour of the mixture has changed from bright orange to pale green. The solvent was removed under reduced pressure and the residue was stirred in 10 ml of n-hexane The pale green solid was collected by filtration (G3) and dried under vacuum. Yield 76%, m.p. 240 °C (dec.). FD-MS: m/z 767 $[M^+ - SbF_6]$. *Anal.* Calc. for $C_{40}H_{43}F_6O_5P_2RuSb$ (1002.5): C, 47 92; H, 4.32; F, 11.37; Ru, 10.08. Found: C, 47.76; H, 4.42; F, 11.08; Ru, 10.34%. IR (KBr): ν(CO) 1976; ν(SbF) 659 cm^{-1}.

Results and discussion

Syntheses of $Cp^*RuCl(P \sim O)_2$ (3a–e)

Oligomeric $[Cp^*RuCl_2]_n$ (**1**) [11, 12] has been described as an excellent precursor for the preparation of Cp^*RuClL_2 complexes (L = tertiary phosphine) in the literature of the last few years [12–16]. The reduction of Ru(III) in **1** was achieved either by prolonged heating of **1** with excess phosphine in absolute ethanol [14] or by treatment of **1** with phosphine in benzene in the presence of Zn as reported by Morris and co-workers [15, 16]. Thus, very long reaction times for the generation of (pentamethylcyclopentadienyl) ruthenium(II) complexes are required following the first pathway [14]. In analogy to the second method we obtained **3a–e** by reaction of the ether-phosphines **2a–e** (Scheme 1) with **1** in toluene and additional Zn (Scheme 2). The chloro complexes $Cp^*RuCl(P \sim O)_2$ (**3a–e**) are air-stable yellow compounds which are very soluble in organic solvents.

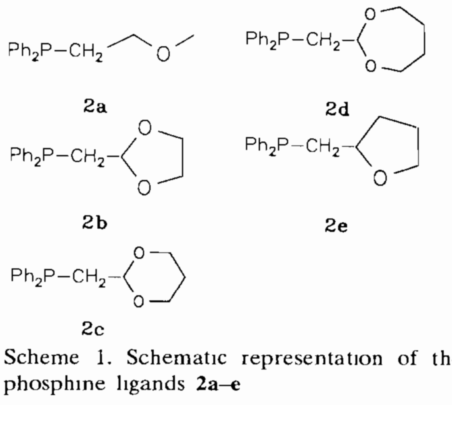

Scheme 1. Schematic representation of the employed ether-phosphine ligands **2a–e**

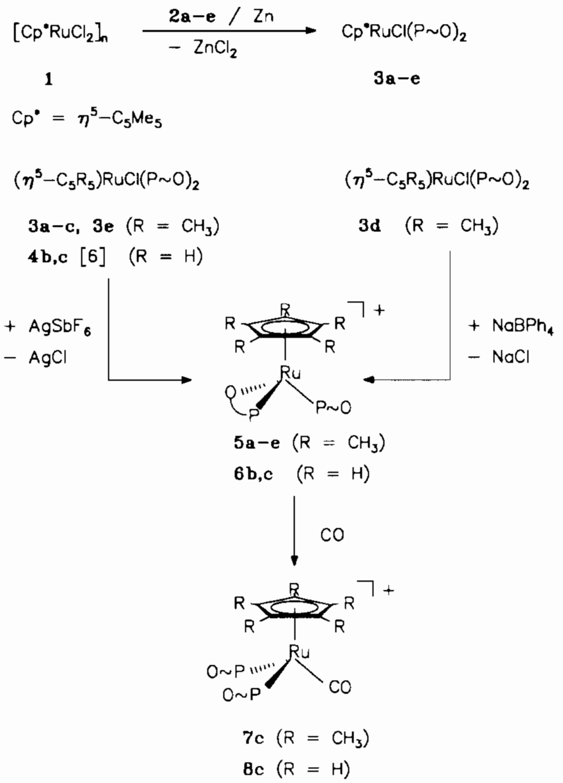

Scheme 2. Schematic representation of the synthesis of the various types of (ether-phosphine)ruthenium(II) complexes P ~ O η^1-P-coordinated; O⌒P η^2-O,P-coordinated

Spectroscopic data and steric properties of 3a–d

The ^{13}C NMR spectra of **3a–d** measured at 22 °C are comparable to related $CpRuCl(P \sim O)_2$ complexes [6]. In addition a singlet due to the CH_3 groups of the Cp* ring is shown in the narrow range 9.2–9.3 ppm. In the IR spectra the antisymmetric C–O–C vibration of the ether moiety is observed as a significant single band in the range 1105–1127 cm^{-1}. However, the ^{31}P NMR spectra (Table 1) indicate the difference between Cp or bulky Cp* ligand in these systems. At −80 °C the complexes **3a–d** display an AB pattern resulting from two different phosphorus atoms. When the temperature is raised the two resonances begin to broaden finally averaging to a single peak at room temperature. This phenomenon may be explained with a hindered rotation about the Ru–P bond due to the steric strain of the Cp* ligand. A similar observation was reported by Mynott *et al.* via ^{13}C NMR spectroscopic studies investigating (cyclopentadienyl)bis(phosphine)ruthenium(II) complexes which contain π-alkene ligands [25]. The ^{13}C NMR spectrum of **3a** recorded at −80 °C (20.15 MHz) shows only broad signals for all carbon atoms of the ether-phosphine ligands but sharp resonances for the C atoms of the C_5Me_5 ring indicating free motion of the Cp* substitutent but a slow rotation rate of the O,P ligand on the ^{13}C NMR time scale. The inequivalency of the two phosphorus atoms is also observed in the solid state, which was demonstrated by two single resonances at 39.3 and 33.5 ppm in the ^{31}P CP-MAS NMR spectrum of **3d**. A temperature dependent ^{31}P NMR spectroscopic study of complex **3d** in toluene was carried out to determine the barrier of Ru–P rotation $\Delta G_c^{\neq}$. Using DNMR5 [22] and ACTPAR [23] the obtained values are as follows: $T_c = 250$ K; $\Delta G_{250}^{\neq} = 47.3 \pm 1.4$ kJ mol^{-1} (with the required law of propagation of errors); $\Delta H^{\neq} = 38.7 \pm 1.0$ kJ mol^{-1}; $\Delta S^{\neq} = -34.3 \pm 3.9$ J mol^{-1} K^{-1}.

*Diastereomers of Cp*RuCl(P ~ O)$_2$ (3e)*

Two diasteromeric forms for complex **3e** occur due to the stereogenic β carbon centre of the ether-phosphine ligand **2e**. If the ruthenium is coordinated by stereochemical different (*RS*/*SR*) phosphines, the metal centre is asymmetric. Its configuration is given by the order of *R* and *S* O,P ligands according to the sequence rules [26, 27]. In this case two enantiomeric forms $R_PS_{Ru}S_P$ and $S_PR_{Ru}R_P$ are obtained which cannot be determined by spectroscopic means. Moreover the two phosphorus atoms in both enantiomers are equivalent. This results from an intramolecular mirror plane producing a singlet at 35.0 ppm in the ^{31}P NMR spectrum (Table 1). Coordination of two stereochemical equivalent (*RR*/*SS*) phosphines to the ruthenium atom leads also to two enantiomers. In spite of the equivalent handedness of both phosphorus fragments, the ^{31}P chemical shifts are inequivalent due to the absence of an intramolecular mirror plane, thus showing an AB pattern at 38.4 and 31.8 ppm in the ^{31}P NMR spectrum (Table 1). The ^{13}C NMR spectrum displays multiplets for all carbon atoms which cannot be assigned unequivocally.

TABLE 1 ^{31}P NMR data[a] of complexes **3a–e**, **5a–e**, **6b,c**, **7c**, **8c**

Complex	T (°C)	δ (ppm)	$^2J_{PP}$ (Hz)
3a	−80	34.0(d), 27.6(d)[b]	42.7
3b	−80	36.0(d), 29.3(d)[c]	43.6
3c	−80	38.3(d), 29.9(d)[c]	42.7
3d	−80	37.9(d), 31.3(d)[c]	43.4
3e	33	38.4(d), 31.8(d)[c]	43.1
		35.0(s)[c]	
5a	−30	51.2(d), 31.7(d)[d]	33.8
5b	−54	59.2(d), 26.9(d)[d]	32.5
		47.5(d), 30.9(d)[d]	32.5
5c	−90	43.4(d), 31.0(d)[d]	31.9
5d	−63	43.3(br)[e], 32.3(d)[d]	33.9
5e	−30	52.0(d), 31.4(d)[d]	33.9
		48.3(d), 35.8(d)[d]	35.3
6b	−30	65.5(d), 29.3(d)[d]	35.1
		48.6(d), 30.2(d)[d]	36.6
6c	−30	65.7(d), 31.7(d)[d]	35.1
		40.4(d), 30.8(d)[d]	36.6
7c	−30	32.1(s)[b]	
8c	−30	31.2(s)[b]	

[a] 32.44 MHz [b] In CH_2Cl_2. [c] In toluene [d] In THF [e] $\omega_{1/2} \approx$ 135 Hz

Monochelated cationic complexes $[(\eta^5\text{-}C_5R_5)Ru(P\sim O)(P\frown O)]^+$ (5a–e, 6b,c)

Starting from neutral Cp*RuCl(P ~ O)$_2$ complexes **3a–e** or already described (cyclopentadienyl)ruthenium(II) complexes **4b,c** it is possible to create an empty coordination site at the ruthenium centre by chloride abstraction, e.g. with $AgSbF_6$ or $NaBPh_4$, respectively (Scheme 2). In this case the ether moiety of one of the monodentate phosphine ligands is able to bind to the ruthenium forming the cationic systems $[(\eta^5\text{-}C_5R_5)Ru(P\sim O)(P\frown O)]^+$ (**5a–e**, **6b,c**). The generation of **5a–c**, **5e**, **6b,c** was performed according to literature methods [6]. By treatment of **3d** with $AgSbF_6$ in THF a decomposition of the desired product was observed to some extent, possibly because of the weakly oxidizing character of the Ag^+ ion. Hence, chloride abstraction was achieved with $NaBPh_4$ in dichloromethane affording $[Cp^*Ru(P\sim O)(P\frown O)][BPh_4]$ (**5d**). All complexes are obtained as orange powders which are air-sensitive in solution. Moreover they are readily soluble in acetone or THF but insoluble in non-polar solvents.

Spectroscopic data of $[Cp^*Ru(P\sim O)(P\frown O)][SbF_6]$ (5a)

The ^{31}P NMR spectrum (Table 1) of **5a** reveals an AB pattern caused by the η^2-O,P chelating and η^1-P coordinated ligands. A band at 1064 cm^{-1} in the IR spectrum is characteristic for η^2-O,P chelation of one ether moiety, while the absorption at 1100 cm^{-1} indicates η^1-P coordination of the second ligand [24].

Spectroscopic and steric properties of $[(\eta^5\text{-}C_5R_5)Ru(P\sim O)(P\frown O)]^+$ (5b–d, 6b,c)

The ^{31}P NMR spectra of the cationic monochelated complexes $[(\eta^5\text{-}C_5R_5)Ru(P\sim O)(P\frown O)]^+$ (**5b–d**, **6b,c**) at low temperatures show that two diastereomers may be formed caused by chirality at the ruthenium centre in addition to C chirality, resulting from η^2-complexation of the O,P ligand (Table 1). Atomic models of complexes **5b–d**, **6b,c** suggest that the steric strain is stronger in the R_MR_C/S_MS_C form than in the R_MS_C/S_MR_C diastereomer, because the cyclic ether moiety interferes with the Cp or Cp* ligand (Scheme 3). A similar observation was reported in the current literature investigating $(\eta^6\text{-}C_6H_6)Os$ complexes which contain op-

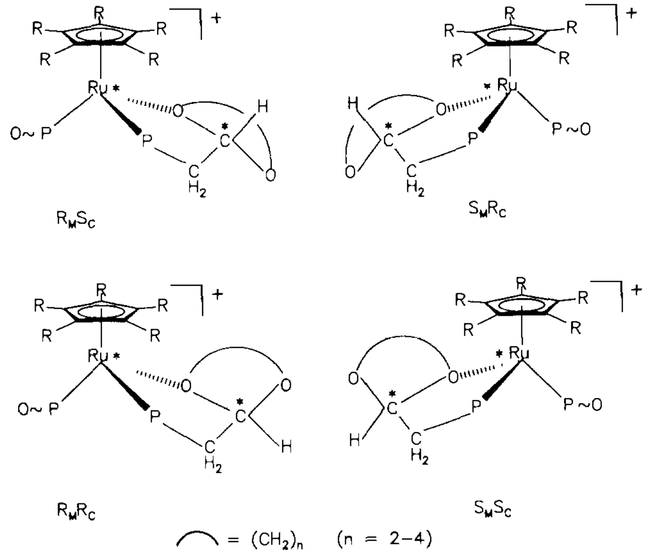

Scheme 3 Possible diastereomeric forms of complexes **5b–d**, **6b,c** caused by C chirality, resulting from the η^2-complexation of the ether-phosphine ligand

tical active aminocarboxylate ligands [28]. However, the presence of the two possible diastereomeric forms is strongly dependent on the employed ether-phosphine ligand and on the η^5-C_5R_5 ligand, respectively. In the complexes **6b,c** containing the Cp ligand both diastereomers were obtained in an approximate 1:1 ratio (Table 1). The low and high field signals in the ^{31}P NMR spectrum can be traced back to the η^2-O,P and η^1-P coordinated ligands. There is a remarkable chemical shift difference between the resonances of the respective η^2-O,P chelating ligands of the two diastereomers (65.5 and 48.6 ppm for **6b**; 65 7 and 40.4 ppm for **6c**) In the case of **5b** both diastereomers can be observed in the ^{31}P NMR spectrum in an approximate 9:1 ratio. The main diastereomer shows signals at 59.2 and 26.9 ppm due to η^2-O,P and η^1-P coordinated ligands, respectively (Table 1). Complexes **5c,d** which contain the bulkier ether-phosphines **2c,d** exhibit one AB pattern at low temperature indicating that only one diastereomer is present which is reasonable interpreted as the sterically favoured R_MS_C/S_MR_C form. The resonance of the η^2-chelating phosphorus atom in these complexes can be observed at relatively high field compared to the corresponding η^2-O,P coordinated phosphorus atom of the main diastereomer of **5b**. Hence, due to the use of the less bulky O,P ligand **2b** complex **5b** obviously seems to contain the sterical stronger R_MR_C/S_MS_C form as the main product. The IR spectra of **5b–d**, **6b,c** show typical bands in the ranges 1066–1075 and 1105–1128 cm^{-1} which can be assigned to the antisymmetric C_2O ether vibration of the η^2-O,P chelating and η^1-P coordinated ligand, respectively.

Spectroscopic data of diastereomeric forms of $[Cp^*Ru(P\sim O)(P^\frown O)][SbF_6]$ (5e)

Chloride abstraction from diastereomeric $Cp^*RuCl(P\sim O)_2$ (**3e**) containing the chiral ether-phosphine ligand **2e** affords cationic monochelated $[Cp^*Ru(P\sim O)(P^\frown O)][SbF_6]$ (**5e**). Due to three chiral centres in this molecule four diastereomeric forms are expected. However, the ^{31}P NMR spectrum of **5e** demonstrates the presence of only two diastereomers (Table 1). Further classification of this system was achieved by a 2D-(P,P)-chemical shift-COSY spectrum showing an AB pattern with resonances at 52.0 and 31.4 ppm and an A'B' pattern at 48.3 and 35.8 ppm, respectively, in an approximate 2:1 ratio Moreover, two absorptions in the IR spectrum at 1066 and 1095 cm^{-1} can be traced back to one η^2-O,P chelating and one η^1-P coordinated ligand.

Dynamic behaviour and variable-temperature ^{31}P NMR studies of 5a–e, 6c

Variable-temperature ^{31}P NMR spectroscopy is an excellent method investigating fluxional processes of transition-metal complexes containing monodentate $(P\sim O)$ and bidentate $(P^\frown O)$ ether-phosphine ligands [6–9]. It is known, that the metal–oxygen bond strength and thus the fluxional behaviour depends on the employed O,P ligands caused by their oxygen basicities and steric constraints [8, 9].

A temperature dependent ^{31}P NMR investigation of the salt $[CpRu(P\sim O)(P^\frown O)][SbF_6]$ (**6c**) containing the weak oxygen basic and bulky O,P ligand **2c** [8] was carried out in the temperature range between −30 and 50 °C. The spectra show line broadening at 10 °C, which is reversible between 10 and 50 °C. At temperatures above 50 °C complex **6c** was dissolved in 1,1',2,2'-tetrachloroethane, but unfortunately decomposition of **6c** took place in this solvent at high temperatures preventing the coalescence temperature to be reached. This behaviour demonstrates a very strong ruthenium–oxygen bond strength caused by the less electron rich ruthenium centre as reported for the corresponding system containing the ether-phosphine ligand **2a** [6]. Referring to this, the only way to labilize the Ru–O bond strength seems to be by increasing the electron density at the ruthenium which is possible by employing a more basic, electron donating pentamethylcyclopentadienyl ligand.

The temperature-dependent ^{31}P NMR spectra of $[Cp^*Ru(P\sim O)(P^\frown O)]^+$ (**5a–e**) indicate that the compounds are fluxional in solution which is regarded as evidence for the decrease of the ruthenium–oxygen bond strength by replacement of Cp versus Cp* in these complexes. The spectra of **5a**, **5c,d** display typical AB patterns at low temperatures, whereas **5b** consists of two diastereomeric forms due to C chirality of the

TABLE 2. Coalescence temperatures and Eyring activation parameters for fluxional processes in **5a–e**

Complex	T_c (K)	$\Delta H^{\neq}$ [a] (kJ mol^{-1})	$\Delta S^{\neq}$ [a] (J mol^{-1} K^{-1})	$\Delta G_c^{\neq}$ [b] (kJ mol^{-1})	$\Delta G^{\neq}$ [c] (kJ mol^{-1})
5d	256	42 4±1.2	−22 7±4 4	48 2±1.6	49.1±1.8
5c	275	43.6±2 7	−26 4±2 7	50 9±3 8	51.5±3 9
5b[d]	274	49.9±2 7	6.8±10 0	48 0±3 8	47.8±4.0
5a	285	51 3±1 1	−3 1±3 8	52 2±1.5	52 3±1 6
5e[e]	320	52.0±2 6	−25.0±8 4	60.0±3 8	59.5±3.6
5e[f]	>325[g]	56 3±2.2	−13.9±7 0	61 0[h]	60.4±3 0

[a] Calculated using a modified version of DNMR5 [22] and ACTPAR [23]. [b] Calculated at T_c using the required law of propagation of errors. [c] Calculated at 298 K using the required law of propagation of errors. [d] Calculation was performed only for the main diastereomer [e] Due to A′B′ pattern. [f] Due to AB pattern. [g] Not obtained due to the boiling point of THF [h] Calculated at 330 K (estimated T_c) using the approximate equation $\Delta G_c^{\neq} = RT_c$ (22 96 + ln $T_c/\delta\nu$)

η^2-O,P chelated ligand. As the temperature is raised, the resonances first broaden, then coalesce (Table 2) with final averaging in sharp singlet in all cases.

In the ^{31}P DNMR spectra of **5c,d** consisting of only one diastereomer (see above), at low temperatures an additional dynamic phenomenon is observed. Below −30 °C the doublet in the high field range due to η^1-P coordinated phosphorus becomes sharp while the signal at lower field caused by the η^2-O,P chelated ligand remains broad or nearly disappears in the base line. Whereas in complex **5c** the broad signal is changing into a sharp doublet at −90 °C, it cannot be resolved in the case of **5d** until −100 °C (Table 1). A rotation around the C–C bond which would lead to an exchange in the coordination of the two oxygen atoms of the chelating O,P ligand would require the dissociation of the metal–oxygen bond. This has been shown to have an energy barrier which is higher (Table 2) than the exchange process responsible for the line broadening of the low field part of the AB pattern. Thus the low energy dynamics may be attributed to conformational changes of the six- and seven-membered ether rings which are coordinated to the ruthenium centre. The ^{31}P NMR spectrum of **5e** shows one AB and one A′B′ pattern at −30 °C due to two diastereomeric forms. When the temperature is raised, the resonances of the diastereomers begin to broaden but with different rate constants k_1/k_2. At 320 K coalescence of the A′B′ pattern is achieved in contrast to the AB pattern which consists of two broad signals until 325 K (Fig. 1). Due to the boiling point of THF a temperature above 325 K was not available.

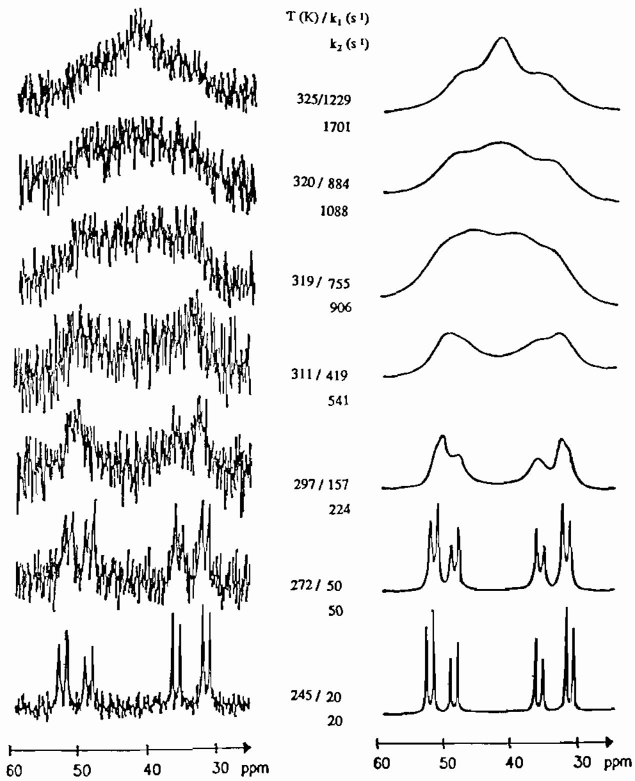

Fig. 1. Experimental and computer-simulated variable-temperature ^{31}P NMR spectra and rate constants (k_1/k_2) for O,P exchange in **5e**

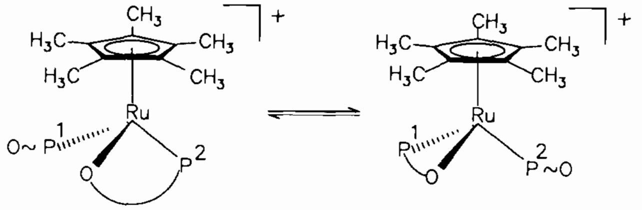

Scheme 4. Mechanism of fluxionality of the complexes $[\mathrm{Cp^*Ru(P{\sim}O)(P^{\frown}O)}]^+$ (**5a–e**)

The temperature data of compounds **5a–e** reveal an averaging of magnetic environments on the NMR time scale at higher temperatures indicating mutual exchange of the two O,P ligands. The exchange mechanism shown in Scheme 4 involves primarily cleavage of the Ru–O bond followed by recombination of the Ru–O bond by the oxygen atom of the second ether-phosphine ligand. All phenomena are reversible.

Additional measurements of **5a–e** in CH_2Cl_2 at low temperatures show similar line shapes and nearly the same chemical shifts. Hence, a strong coordination of the THF molecule to the fluxional system can be excluded.

Using DNMR5 [22], computer-generated spectra were obtained and iteratively fitted to the experimental spectra in order to evaluate the rate constants for the exchange process at different temperatures Graphic application of the Eyring equation to the kinetic data involving a non-linear least-squares program (ACTPAR [23]) afforded the thermodynamic parameters $\Delta H^{\neq}$, $\Delta S^{\neq}$, $\Delta G_c^{\neq}$ and $\Delta G_{298}^{\neq}$ (Table 2). In all cases the entropies show small positive or negative values indicating an intramolecular exchange [8]. The difference between the ground-state and transition-state energies is reflected by $\Delta G^{\neq}$, while $\Delta H^{\neq}$ may be best interpreted as an indication of the Ru–O bond strength. The calculated values of $\Delta H^{\neq}$ in **5a–e** exhibit that ether-phosphines **2a,e** form a stronger Ru–O contact than the O,P ligands **2b–d** with two oxygen donors in 1,3-position in these systems. Thus, the Ru–O bond strength in complexes **5b–d** is decreased with increase of the ring size of the cyclic ether moiety because bulky O,P ligands are able to cause steric destabilization of the ground state relative to the transition state, hence reducing the barriers of fluxionality [8]. Complex **5e** with the strong basic ether-phosphine ligand **2e** gives two different $\Delta H^{\neq}$ values due to the two diastereomeric forms.

Preparation and spectroscopic data of $[(\eta^5\text{-}C_5R_5)Ru(P\sim O)_2(CO)][SbF_6]$ (7c, 8c)

Cleavage of the ruthenium–oxygen contact in cationic monochelated complexes $[(\eta^5\text{-}C_5R_5)Ru(P\sim O)(P^\frown O)][SbF_6]$ (**5c**, **6c**) takes place by reaction with strong donor–acceptor ligands, e.g. carbon monoxide. If **5c**, **6c** are stirred under an atmosphere of CO at ambient temperature, a colour change of the reaction mixture indicates the formation of the stable complexes $[(\eta^5\text{-}C_5R_5)Ru(P\sim O)_2(CO)][SbF_6]$ (**7c**, **8c**) (Scheme 1). The completion of the reaction is detected by ^{31}P NMR spectroscopy. Whereas in the case of **5c** the corresponding carbon monoxide complex **7c** was obtained after only 10 min, a reaction time of approximately 12 h is required for **6c** (Table 1). These differences in reactivity demonstrate the increase of electron density at ruthenium and thus the decrease of the Ru–O bond strength on replacing Cp by Cp*. **7c** and **8c** show a single absorption in the IR spectrum at 1946 and 1976 cm^{-1}, respectively.

Acknowledgements

The support of this research by the Fonds der Chemischen Industrie is gratefully acknowledged. We thank the BASF Aktiengesellschaft for starting materials and Professor U. Nagel and Dr B Rieger for helpful discussions.

References

1 S.G Davies, J.P McNally and A J. Smallridge, *Adv Organomet Chem*, *30* (1990) 1, and refs therein.
2 T Blackmore, M.I Bruce and F G.A. Stone, *J Chem Soc A*, (1971) 2376
3 G. Consiglio and F. Morandini, *Chem Rev*, *87* (1987) 761.
4 F L Joslin, M P Johnson, J.T Mague and D M Roundhill, *Organometallics*, *10* (1991) 2781
5 M.I Bruce and F S Wong, *J Organomet Chem*, *210* (1981) C5
6 B. de Klerk-Engels, J.H Groen, K Vrieze, A Mockel, E Lindner and K Goubitz, *Inorg Chim Acta*, *195* (1992) 237
7 A Bader and E Lindner, *Coord Chem Rev*, *108* (1991) 27, and refs therein.
8 E. Lindner, A Mockel, H A. Mayer, H Kuhbauch, R Fawzi and M Steimann, *Inorg Chem*, *32* (1993) 1266
9 E. Lindner, J. Dettinger, H A Mayer, R Fawzi and M Steimann, *Chem Ber*, *126* (1993) 1317
10 R Poli, *Chem Rev*, *91* (1991) 509
11 T D Tilley, R H Grubbs and J E Bercaw, *Organometallics*, *3* (1984) 274
12 N. Oshima, H Suzuki and Y Moro-Oka, *Chem Lett*, (1984) 1161
13 H. Lehmkuhl, M Bellenbaum, J Grundke, H Mauermann and C. Kruger, *Chem Ber*, *121* (1988) 1719
14 M.S. Chinn and D M Heinekey, *J Am Chem Soc*, *112* (1990) 5166.
15 G. Jia and R H Morris, *J Am Chem Soc*, *113* (1991) 875
16 G Jia, A J Lough and R.H. Morris, *Organometallics*, *11* (1992) 161.
17 (a) W Schoniger, *Microchim Acta*, (1955) 123, (b) (1956) 869
18 A. Dirschel and F Erne, *Microchim Acta*, (1961) 866.
19 G Brunisholz and J Michot, *Helv Chim Acta*, *37* (1954) 589
20 E Lindner, A. Bader and H A Mayer, *Z Anorg Allg Chem*, *598/599* (1991) 235.
21 (a) A L Van Geet, *Anal Chem*, *40* (1968) 2227; (b) *42* (1970) 679
22 The routines of data input and data conversion were modified by Hartwig Kuhbauch, Universitat Tubingen, Germany 1992
23 G Binsch and H Kessler, *Angew Chem*, *Int Ed Engl*, *19* (1980) 411, and refs therein
24 E. Lindner, J Dettinger and A. Mockel, *Z. Naturforsch*, *Teil B*, *46* (1991) 1519
25 R. Mynott, H Lehmkuhl, E-M Kreuzer and E Joussen, *Angew Chem*, *Int Ed Engl*, *29* (1990) 289.
26 (a) R S Cahn, C Ingold and V Prelog, *Angew Chem*, *Int Ed Engl*, *5* (1966) 385, (b) V. Prelog and G Helmchen, *Angew Chem*, *Int. Ed Engl*, *21* (1982) 567.
27 (a) K Stanley and M C Baird, *J Am Chem Soc*, *97* (1975) 6598, (b) H Brunner, *Adv Organomet Chem*, *18* (1980) 151
28 H Werner, T Daniel, O. Nurnberg, W Knaup and U Meyer, *J Organomet Chem*, *445* (1993) 229